



The “ λ -medial axis”

Frédéric Chazal^a, André Lieutier^{b,c,*}

^a *Institut de Mathématiques de Bourgogne, Université de Bourgogne, UMR 5584, UFR des Sciences et Techniques, 9 Avenue Alain Savary, B.P. 47870, 21078 Dijon Cedex, France*

^b *Dassault Systèmes, 53 Avenue de l'Europe, 13082 Aix-en-Provence Cedex 2, France*

^c *LMC/IMAG Grenoble, France*

Received 29 April 2004; received in revised form 6 December 2004; accepted 14 January 2005

Abstract

Medial axis is known to be unstable for nonsmooth objects. For an open set \mathcal{O} , we define the *weak feature size*, *wfs*, minimum distance between \mathcal{O}^c and the critical points of the function distance to \mathcal{O}^c . We introduce the “*lambda-medial axis*” \mathcal{M}_λ of \mathcal{O} , a subset of the medial axis of \mathcal{O} which captures the homotopy type of \mathcal{O} when $\lambda < \text{wfs}$. We show that, at least for some “regular” values of λ , \mathcal{M}_λ remains stable under Hausdorff distance perturbations of \mathcal{O}^c .

© 2005 Elsevier Inc. All rights reserved.

Keywords: Medial axis; Stability; Homotopy type

1. Introduction and related works

The medial axis \mathcal{M} of an open set \mathcal{O} in \mathbb{R}^n is the set of points $x \in \mathcal{O}$ for which there is at least 2 closest points on the complement \mathcal{O}^c (see Section 2). The medial axis has applications in image analysis and mathematical morphology [30], Solid Modeling [8], or domain decomposition for CAD to CAE (i.e., Finite Elements) models generation [32,33].

* Corresponding author.

E-mail addresses: fchazal@u-bourgogne.fr (F. Chazal), andre_lieutier@ds-fr.com (A. Lieutier).

For a few years, most successful methods for reconstructing a 3D shape from unorganized data points sampled on the shape boundary start with a three-dimensional Voronoi diagram of the points [1–3,9,18]. Recall that, for a finite set of points S , the medial axis of the complement S^c of S is the Voronoi diagram of S , or, more accurately, the union of the cells of dimension at most $n - 1$ in the Voronoi diagram. In the “Power Crust” paper [2], the proposed reconstruction algorithm consists of:

- (1) computing an approximation of the Medial Axis of the shape from the Voronoi diagram of the sampled points,
- (2) reconstructing the Solid corresponding to this approximate Medial Axis, together with the associated distance function.

The approximation of the Medial Axis in step 1 consists of the selection of a subset of the Voronoi vertices, called the poles. It has been shown in [9,2] that, for a C^2 smooth surface, the set of poles converges toward the Medial Axis in Hausdorff distance when the sampling density approaches 0. Even if this is not explicit in other algorithms based on 3D Voronoi diagrams, topological fidelity in reconstruction algorithms is related to the ability to select a relevant subset of the Voronoi diagram of the sampling that approaches the Medial Axis of the underlying object.

The exact computation paradigm assumes exact inputs belonging to countable sets, for which usual geometric predicates are decidable and can then be computed exactly. On the other hand considering approximate inputs (or inputs belonging to uncountable sets) asks for a model of computation in which the continuity (that is the stability) of the operator is required: one should be able to compute an arbitrary accurate approximation of the output using a sufficiently accurate approximation of the input. Proposed algorithms for the computation of the Medial axis in the first model of computation includes Voronoi diagram of a finite set of rational points, and seems to be feasible for exact (that is rational or algebraic numbers) polyhedral inputs (see [14,19,20]).

For nonexact inputs, such as CAD BRep models or measured objects, one has to do with approximation. The computation of the Medial Axis of two-dimensional or three-dimensional solids is known to be problematic due to its unstableness: small variations in the boundary of an object result in large variations of its Medial Axis. For example, if the input is a BRep solid, an arbitrary small G^0 (incidence) or G^1 (tangency) discontinuity between two boundary elements entails a large “spike” in the Medial Axis. We would like to emphasize here that this unstableness is not a technical difficulty related to a specific algorithm: when the output is not a continuous function of the input, the result of any computation is meaningless, unless assuming “exact” input data, which is not realistic for measured or even usual CAD data. Following the ideas developed for surface reconstruction algorithms, some authors have examined how a specific subset of the Voronoi complex of the sampled points can be used as an approximation of the Medial axis [2,15,16]. These approaches assume that the sampled points lie *exactly* on a smooth surface with a positive lfs. The lfs is the minimal distance from the boundary to the Medial Axis and gives an upper bound on the curvature for a C^2 surface. Indeed, in order to

approximate the Medial Axis with respect to the Hausdorff distance, one needs informations about the boundary both in position, tangency, and curvature (see [10]). These informations are in a sense hidden in the assumptions of positive lfs and exact sampling. However, regarding the sampling informations actually available and the kind of solids encountered in real life, one should be able to achieve reasonable approximations with weaker assumptions. *The aim of this work is to understand what kind of approximation one can obtain with a priori minimum assumptions on the regularity of the solid boundary or on the quality of the sampling.*

We consider a general class of objects (namely the open bounded subsets of \mathbb{R}^n) and we replace the notion of sampling by the more general class of closed sets approximating the boundary within a given Hausdorff distance. Practically, this point of view allows considering noised sampling of nonsmooth objects. Of course, without any information on the existence of tangent planes or bounded curvature, one cannot expect to find a good Hausdorff distance approximation of the Medial Axis. Instead, we are looking to another object, \mathcal{M}_λ , subset of the Medial Axis. \mathcal{M}_λ is the set of points for which any ball containing the set of closest points on the boundary has radius at least λ .

Beyond the Medial Axis, the distance function to the complement induces in fact a finer structure. In [27], the homotopy equivalence of any open bounded subset of \mathbb{R}^n with its Medial Axis has been proved using a continuous deformation flow. This flow integrates, in some weakened sense, a discontinuous vector field ∇ which is an extension of the gradient of the distance function. Intuitively, for a point $x \in \mathcal{O}$, $\nabla(x)$ gives the local direction to go in order to optimally increase the distance to the complement, while its norm is the rate of growth of this distance when moving in this direction (see Section 2). This flow has been independently introduced in [17,18,25] in the particular situation where the complement \mathcal{O}^c of \mathcal{O} is finite (i.e., for Voronoi diagrams). These authors have shown that the Flow Diagram induces a nice structure on the Voronoi diagram. According to [27], this flow and the associated structures remain valid for general open sets. These structures rely in particular on the *critical points* of this flow, that is the set of points x for which $\nabla(x) = 0$, as well as the stable/unstable manifolds [18,25] associated to these critical points.

We introduce the weak feature size, wfs, minimum distance between \mathcal{O}^c and the critical points of \mathcal{O} . We show in Section 3 that performing an erosion of distance d on \mathcal{O} , that is removing from \mathcal{O} any point at distance at most d from \mathcal{O}^c , preserves the homotopy type of \mathcal{O} as far as $d < \text{wfs}$. \mathcal{M}_λ enjoys the property of capturing the homotopy type of the object when $\lambda < \text{wfs}$ and, when $\lambda < \text{wfs}$ its homotopy corresponds to a filtered homotopy that ignores topological features smaller than λ (Section 3).

The critical points of ∇ and the weak feature size are closely related to the theory of critical points of distance functions [26,23]. Such a theory allows to deduce several properties of the objects studied in this paper. In particular, one proves that most of the open sets encountered in practical situations (piecewise analytic open sets) have a positive weak feature size. One also shows that to any open set \mathcal{O} with positive wfs, one can associate in a canonical way a topological manifold which approximate the boundary of \mathcal{O} . These results are given in Section 3.4.

We claim that \mathcal{M}_λ is more relevant than \mathcal{M} in most practical situations because it remains stable and well defined without any assumption on the smoothness of the object or of an unlikely exactness of the sampling. Section 5 examines in which precise sense the \mathcal{M}_λ of the “exact object” can be approximated from the \mathcal{M}_λ of its Hausdorff approximation, therefore giving a sound foundation of any computation of this object in realistic situations, which is proved hopeless for the Medial Axis. It also gives a straightforward algorithm using filtered Voronoi diagrams of sampled points as approximations (see Section 5.1)

2. Definitions

2.1. The continuous deformation \mathfrak{C}

We use the following definitions and notations. In the whole paper, \mathcal{O} and \mathcal{M} always denote, respectively, a bounded open subset of \mathbb{R}^n and its Medial Axis defined below. For any set X , \bar{X} , X° , ∂X , and X^c denote, respectively, the closure, the interior, the boundary, and the complement of X . $\mathbb{B}_{x,r}$ and $\mathbb{B}_{x,r}^\circ$, respectively, denote the closed and open ball of center x and radius r in \mathbb{R}^n . We denote by $\mathbb{S}_{x,r}$ the corresponding sphere, that is $\mathbb{S}_{x,r} = \mathbb{B}_{x,r} \setminus \mathbb{B}_{x,r}^\circ$.

For any point $x \in \mathcal{O}$, we denote by $\Gamma(x)$ the set of closest boundary points, that is:

$$\begin{aligned} \Gamma(x) &= \{y \in \mathcal{O}^c, d(x, y) = d(x, \mathcal{O}^c)\} \\ &= \{y \in \partial\mathcal{O}, d(x, y) = d(x, \partial\mathcal{O})\}. \end{aligned}$$

Because $\partial\mathcal{O}$ is compact, $\Gamma(x)$ is a nonempty compact set. For a set E , $|E|$ denotes the cardinal of E .

Definition 2.1. (Medial Axis) The Medial Axis \mathcal{M} of the open set \mathcal{O} is the set of points x of \mathcal{O} who have at least 2 closest boundary points:

$$\mathcal{M} = \{x \in \mathcal{O}, |\Gamma(x)| \geq 2\}.$$

The strictly positive, real valued function \mathcal{R} defined on \mathcal{O} is the distance to the boundary.

$$\mathcal{R}(x) = d(x, \mathcal{O}^c).$$

One can check, using the triangular inequality twice, that \mathcal{R} is 1-Lipschitz.

There always exists a unique closed ball with minimal radius enclosing $\Gamma(x)$. The existence follows from the compactness of the set of balls whose radius is bounded by a given value B and containing $\Gamma(x)$ and the uniqueness from the fact that if two distinct balls contain $\Gamma(x)$ there exist another ball of strictly smaller radius enclosing it. The real valued, positive function \mathcal{F} is defined as the radius of this smallest closed ball enclosing $\Gamma(x)$ (cf. Fig. 1). In other words:

$$\mathcal{F}(x) = \inf\{r, \exists y \in \mathbb{R}^n, \mathbb{B}_{y,r} \supset \Gamma(x)\}.$$

One proves in [27] that \mathcal{F} is *upper semicontinuous*, that is:

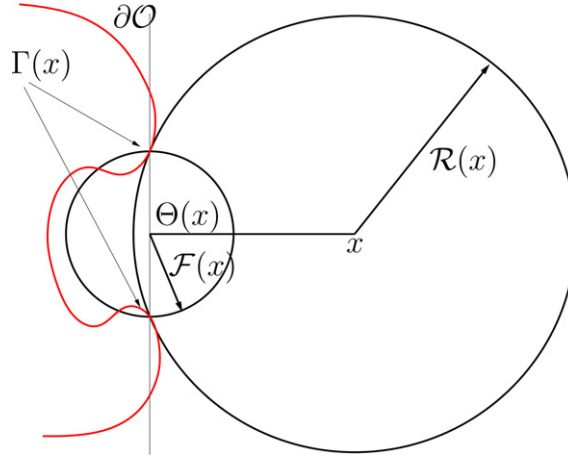


Fig. 1. A two-dimensional example with two closest points.

$\forall \epsilon \in \mathbb{R}, \{x \in \mathcal{O}, \mathcal{F}(x) < \epsilon\}$ is open.

Similarly, $\Theta(x)$ denotes the center of this smallest enclosing ball. Of course, when $x \notin \mathcal{M}$, we have $\Gamma(x) = \{\Theta(x)\}$ and $\mathcal{F}(x) = 0$.

The vector function ∇ extends the gradient of \mathcal{R} . $\nabla(x)$ is defined for all $x \in \mathcal{O}$ and coincides with the gradient of \mathcal{R} when $x \in \mathcal{O} - \overline{\mathcal{M}}$. It is defined as follows:

$$\nabla(x) = \frac{x - \Theta(x)}{\mathcal{R}(x)}.$$

One has the following relation (see [27]):

$$\nabla(x)^2 = 1 - \frac{\mathcal{F}(x)^2}{\mathcal{R}(x)^2}. \quad (1)$$

The map $x \mapsto \|\nabla(x)\|$ is lower semicontinuous (see [27]). The *critical points* of ∇ are the points x for which $\nabla(x) = 0$. When \mathcal{O}^c is finite, that is for Voronoi diagrams, critical points are the intersections of the Delaunay cells with their dual Voronoi cell (when they do intersect). In the general case, a point x is a critical point if and only if it lies in the convex hull of $\Gamma(x) : x \in \mathcal{CH}(\Gamma(x))$.

∇ is not continuous. However, it is shown in [27] that Euler schemes using this vector fields converge uniformly, when the integration step decreases, toward a continuous flow \mathfrak{C} :

$$\mathfrak{C} : \mathbb{R}^+ \times \mathcal{O} \mapsto \mathcal{O}.$$

This flow realizes the homotopy equivalence (see Section 2.2) between \mathcal{O} and \mathcal{M} .

One proves in [27] the following equalities:

$$\mathfrak{C}(t, x) = x + \int_0^t \nabla(\mathfrak{C}(\tau, x)) d\tau, \quad (2)$$

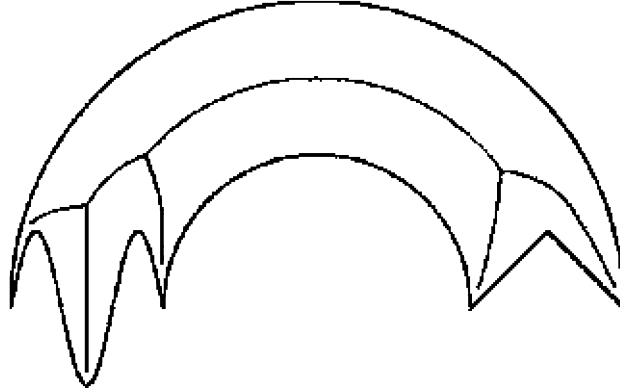


Fig. 2. Example of \mathcal{M}_λ with $\lambda = 0.1$.

$$\mathcal{R}(\mathfrak{C}(t, x)) = \mathcal{R}(x) + \int_0^t \nabla(\mathfrak{C}(\tau, x))^2 d\tau. \quad (3)$$

The curve image of $t \mapsto \mathfrak{C}(t, x)$ is rectifiable and its arc length is an increasing function of t given by:

$$s(t) = \int_0^t \|\nabla(\mathfrak{C}(\tau, x))\| d\tau \quad (4)$$

and, if one denotes $s \mapsto t(s)$ the inverse map:

$$\mathcal{R}(\mathfrak{C}(t(s), x)) = \mathcal{R}(x) + \int_0^s \|\nabla(\mathfrak{C}(t(\sigma), x))\| d\sigma. \quad (5)$$

The main object studied in the paper, \mathcal{M}_λ is defined by (see Fig. 2 for an example):

$$\mathcal{M}_\lambda = \{x \in \mathcal{O}, \mathcal{F}(x) \geq \lambda\}.$$

Notice that, because \mathcal{F} is upper semicontinuous \mathcal{M}_λ is a closed set.

2.2. Homotopy equivalence

Two maps $f_0 : X \mapsto Y$ and $f_1 : X \mapsto Y$ are said *homotopic* if there is a continuous map H , $H : [0, 1] \times X \mapsto Y$, such that $\forall x \in X, H(0, x) = f_0(x)$ and $H(1, x) = f_1(x)$.

The homotopy equivalence between topological sets enforces a one to one correspondence between connected components, cycles, holes, tunnels, cavities, or higher dimensional topological features of the two sets, as well as the way these features are related.

The definition of homotopy equivalence can be found in [24, pp. 171–172] or [31, p. 108]:

Two spaces X and Y are said to have the same homotopy type if there are continuous maps $f : X \mapsto Y$ and $g : Y \mapsto X$ such that $g \circ f$ is homotopic to the identity map of X and $f \circ g$ is homotopic to the identity map of Y .

We are in the case where $Y \subset X$ and g is the canonical inclusion: $\forall y \in Y, g(y) = y$. In Section 3, as in [27], the homotopy equivalence is proved using the following characterization. The definition of a deformation retract given below is taken from [29, p. 66].

Proposition 2.2. *If $Y \subset X$ and there exists a continuous map $H, H: [0, 1] \times X \mapsto X$ such that:*

- $\forall x \in X, H(0, x) = x$
- $\forall x \in X, H(1, x) \in Y$
- $\forall y \in Y, \forall t \in [0, 1], H(t, y) \in Y$

then, X and Y have same homotopy type. If one replaces the third property by the stronger one: $\forall y \in Y, \forall t \in [0, 1], H(t, y) = y$, H defines a deformation retract of X towards Y .

2.3. Hausdorff distance

Hausdorff distance between sets will be widely used in the paper. Basic definitions and properties of this distance are quickly recalled. For more general results and detailed proofs, the reader is referred to [5, Section 9.11] for example.

Definition 2.3. Let A and B be two compact subsets of \mathbb{R}^n . The Hausdorff distance between A and B is defined by

$$d_H(A, B) = \max \left(\sup_{x \in A} d(x, B), \sup_{y \in B} d(y, A) \right).$$

Hausdorff distance defines a distance on the set $\mathcal{K}(\mathbb{R}^n)$ of compact subsets of \mathbb{R}^n which becomes a complete metric space. Moreover, if K is some fixed compact set, the metric space $(\mathcal{K}(\mathbb{R}^n)_K, d_H)$ of compact subsets contained in K is compact.

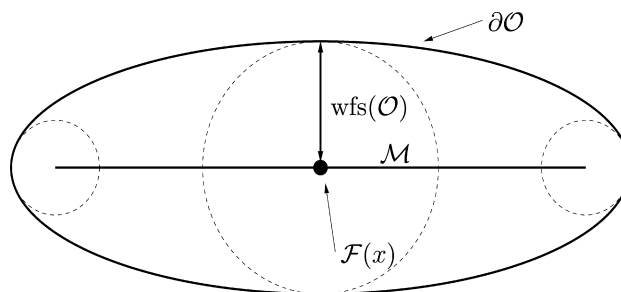


Fig. 3. Weak feature size of an ellipse.

3. Homotopy type of $\mathcal{M}_\lambda(\mathcal{O})$

Definition 3.1. The *Weak Feature Size*, denoted $\text{wfs}(\mathcal{O})$, of an open, bounded subset \mathcal{O} of \mathbb{R}^n is the distance between the complement \mathcal{O}^c and the set of critical points $\{x \in \mathcal{O}, \nabla(x) = 0\}$ of the distance function. Fig. 3 shows the Weak Feature Size of an ellipse.

In this section, we show that, if $\lambda < \text{wfs}(\mathcal{O})$, then $\overline{\mathcal{O}_\lambda} = \{x \in \mathcal{O}, \mathcal{R}(x) \geq \lambda\}$, is a deformation retract of \mathcal{O} (Theorem 1) and that $\mathcal{M}_\lambda(\mathcal{O})$ carries the homotopy type of \mathcal{O} (Theorem 2).

3.1. Definition of $\mathbf{F}_\beta(\mathcal{O})$, $\mathbf{G}_\beta(\mathcal{O})$ and first properties

We denote by \mathcal{O} an open, bounded subset of \mathbb{R}^n . The set of critical points of the vector field ∇ , $\{x \in \mathcal{O}, \nabla(x) = 0\}$, or, equivalently, the set of *fix points* of the map $x \mapsto \mathfrak{C}(t, x)$ will be denoted by $\mathbf{F}(\mathcal{O})$. More generally, we introduce the set $\mathbf{F}_\beta(\mathcal{O})$:

$$\mathbf{F}_\beta(\mathcal{O}) = \{x \in \mathcal{O}, \|\nabla(x)\| \leq \beta\}.$$

With this notation, one has of course $\mathbf{F}_0(\mathcal{O}) = \mathbf{F}(\mathcal{O})$. Because the map $x \mapsto \|\nabla(x)\|$ is lower semi-continuous, $\mathbf{F}_\beta(\mathcal{O})$ is a closed set for the relative topology in \mathcal{O} . One has of course $\beta \leq \beta' \Rightarrow \mathbf{F}_\beta(\mathcal{O}) \subset \mathbf{F}_{\beta'}(\mathcal{O})$. Notice that $\mathbf{F}_\beta(\mathcal{O})$ is related to the filtering of the Voronoi diagram by angle criterion, taking β as the cos of the angle [22]. However, when $\beta > 0$, $\mathbf{F}_\beta(\mathcal{O})$ is not, in general, globally invariant by the action of $x \mapsto \mathfrak{C}(t, x)$ and, therefore does not, in general, keep the homotopy type of \mathcal{O} .

We introduce now $\mathbf{G}_\beta(\mathcal{O})$, the *smallest superset of $\mathbf{F}_\beta(\mathcal{O})$ that is globally invariant by the action of $x \mapsto \mathfrak{C}(t, x)$* :

$$\begin{aligned} \mathbf{G}_\beta(\mathcal{O}) &= \mathfrak{C}(\mathbb{R}^+, \mathbf{F}_\beta(\mathcal{O})) \\ &= \{x \in \mathcal{O}, \exists t \in \mathbb{R}^+, \exists y \in \mathbf{F}_\beta(\mathcal{O}), x = \mathfrak{C}(t, y)\}. \end{aligned}$$

One has of course $\mathbf{F}_\beta(\mathcal{O}) \subset \mathbf{G}_\beta(\mathcal{O})$ and $\beta \leq \beta' \Rightarrow \mathbf{G}_\beta(\mathcal{O}) \subset \mathbf{G}_{\beta'}(\mathcal{O})$. Unlike $\mathbf{F}_\beta(\mathcal{O})$, $\mathbf{G}_\beta(\mathcal{O})$ carries the homotopy of \mathcal{O} , as stated in the lemma below.

Lemma 3.2. *Let D be the diameter of \mathcal{O} .*

$$\forall x \in \mathcal{O}, \quad \mathfrak{C}\left(\frac{D}{\beta^2}, x\right) \in \mathbf{G}_\beta(\mathcal{O}).$$

Proof. Let us assume that this is not true for some $x \in \mathcal{O}$:

$$\mathfrak{C}\left(\frac{D}{\beta^2}, x\right) \notin \mathbf{G}_\beta(\mathcal{O})$$

which entails

$$\forall t \in \left[0, \frac{D}{\beta^2}\right], \quad \mathfrak{C}(t, x) \notin \mathbf{F}_\beta(\mathcal{O})$$

that is

$$\forall t \in \left[0, \frac{D}{\beta^2}\right], \quad \|\nabla(\mathfrak{C}(t, x))\| > \beta$$

which gives:

$$\begin{aligned} \mathcal{R}\left(\mathfrak{C}\left(\frac{D}{\beta^2}, x\right)\right) &= \mathcal{R}(x) + \int_0^{\frac{D}{\beta^2}} \nabla(\mathfrak{C}(\tau, x))^2 d\tau \\ &> \mathcal{R}(x) + \int_0^{\frac{D}{\beta^2}} \beta^2 d\tau = \mathcal{R}(x) + D. \end{aligned}$$

which contradicts the definition of D . \square

Lemma 3.3. *For any $\beta > 0$, $\mathbf{G}_\beta(\mathcal{O})$ has the same homotopy type than \mathcal{O} .*

Proof. We use the characterization of Proposition 2.2. From the definition of $\mathbf{G}_\beta(\mathcal{O})$, it is clear that it is globally invariant by the action of $x \mapsto \mathfrak{C}(t, x)$, that is:

$$\forall x \in \mathbf{G}_\beta(\mathcal{O}), \quad \forall t \in \mathbb{R}^+, \quad \mathfrak{C}(t, x) \in \mathbf{G}_\beta(\mathcal{O}).$$

From this property and Lemma 3.2, the homotopy $[0, 1] \times \mathcal{O} \mapsto \mathcal{O}$ defined by $(t, x) \mapsto \mathfrak{C}(t \frac{D}{\beta^2}, x)$ defines an homotopy equivalence between \mathcal{O} and $\mathbf{G}_\beta(\mathcal{O})$. \square

3.2. Introduction of the weak feature size

For two sets A, B we denote by $d(A, B)$ the minimum distance between all the pairs of points in A and B :

$$d(A, B) = \inf_{a \in A, b \in B} d(a, b). \quad (6)$$

Take care that, unlike the Hausdorff distance d_H among compact sets, d does not satisfy the triangular inequality and is therefore not a distance.

Definition 3.4. We call *Weak Feature Size* of \mathcal{O} , denoted by $\text{wfs}(\mathcal{O})$, the distance between \mathcal{O}^c and $\mathbf{F}(\mathcal{O})$:

$$\begin{aligned} \text{wfs}(\mathcal{O}) &= d(\mathcal{O}^c, \mathbf{F}(\mathcal{O})) \\ &= \inf_{x \in \mathbf{F}(\mathcal{O})} \mathcal{R}(x). \end{aligned}$$

In the section below, one focuses on open sets \mathcal{O} with positive wfs . The condition $\text{wfs} > 0$ can be seen as a kind of minimum regularity condition on the boundary of \mathcal{O} . Notice that, even when $\text{wfs} > 0$, $\|\nabla(x)\|$ can be arbitrarily small near $\partial\mathcal{O}$. Consider for example, in \mathbb{R}^2 , the set S :

$$S = \{(x, y) \in \mathbb{R}^2, 0 < x < 1 \text{ and } 0 < y < x^2\}.$$

$\|\nabla(x)\|$ can be arbitrarily small near the point $(0, 0)$. However, there is only one critical point and $\text{wfs}(S) > 0$. In other words, in general, $\text{wfs}(\mathcal{O}) = d(\mathcal{O}^c, \mathbf{F}(\mathcal{O}))$ is not equal to $\sup_{\beta > 0} d(\mathcal{O}^c, \mathbf{F}_\beta(\mathcal{O}))$.

For $\epsilon > 0$ and a set X , one denotes by $X^{+\epsilon}$ the open set of points whose distance to X is strictly smaller than ϵ . One has:

Lemma 3.5.

$$\forall \epsilon > 0, \exists \beta > 0, \mathbf{F}_\beta(\mathcal{O}) \subset (\mathcal{O}^c)^{+\epsilon} \cup \mathbf{F}(\mathcal{O})^{+\epsilon}.$$

Proof. From the definition of $\mathbf{F}_\beta(\mathcal{O})$ one has:

$$\mathbf{F}(\mathcal{O}) = \bigcap_{n \in \mathbb{N}, n \geq 1} \mathbf{F}_n(\mathcal{O}). \quad (7)$$

For any integer $n \geq 1$, the set K_n

$$K_n = \mathbf{F}_n(\mathcal{O}) \setminus ((\mathcal{O}^c)^{+\epsilon} \cup \mathbf{F}(\mathcal{O})^{+\epsilon})$$

is compact. Indeed, $\mathbf{F}_n(\mathcal{O})$ being closed for the relative topology in \mathcal{O} , one get a closed set by removing $(\mathcal{O}^c)^{+\epsilon}$.

The sequence K_n is decreasing for the inclusion order and it results from Eq. (7) that:

$$\bigcap_{n \in \mathbb{N}, n \geq 1} K_n = \emptyset.$$

It results from the compactness of the K_n that, for some integer N , $K_N = \emptyset$ which means:

$$\mathbf{F}_N(\mathcal{O}) \subset (\mathcal{O}^c)^{+\epsilon} \cup \mathbf{F}(\mathcal{O})^{+\epsilon}. \quad \square$$

Let us denote by \mathbf{D}_ϵ the set of points of \mathcal{O} whose distance to the complement (\mathcal{O}^c) is comprised between ϵ and $\text{wfs} - \epsilon$:

$$\mathbf{D}_\epsilon = \{x \in \mathcal{O}, \epsilon \leq \mathcal{R}(x) \leq \text{wfs} - \epsilon\}.$$

From Lemma 3.5, we know that for any $\epsilon > 0$, there exists $\beta > 0$ such that

$$\forall x \in \mathbf{D}_\epsilon, \quad \beta < \|\nabla(x)\| \leq 1. \quad (8)$$

Let x in \mathbf{D}_ϵ and $r \in [0, \text{wfs} - \epsilon - \mathcal{R}(x)]$. We claim that there exists a unique t , $t \in [0, \frac{\text{wfs}}{\beta^2}]$ such that:

$$\mathcal{R}(\mathfrak{C}(t, x)) = \mathcal{R}(x) + r.$$

Indeed, assuming $\mathcal{R}(\mathfrak{C}(\frac{\text{wfs}}{\beta^2}, x)) < \text{wfs} - \epsilon$ leads to a contradiction with Eq. (3) and relation (8). The map $t \mapsto \mathcal{R}(\mathfrak{C}(t, x))$ is continuous and strictly increasing by (3) and (8). Therefore, one get the existence and uniqueness of a such t .

This allows to introduce the map \mathfrak{C}_r :

$$\mathfrak{C}_r(r, x) = \mathfrak{C}(t, x)$$

defined for any $x \in \mathbf{D}_\epsilon$ and $r \in [0, \text{wfs} - \epsilon - \mathcal{R}(x)]$. This means that, for $x \in \mathbf{D}_\epsilon$ and as far as the distance to \mathcal{O}^c is less than $\text{wfs} - \epsilon$, one can parametrize the trajectory of x by the distance r to the complement.

Let us consider $x \in \mathbf{D}_\epsilon$ with $\mathfrak{C}(t_1, x) \in \mathbf{D}_\epsilon$ and $\mathfrak{C}(t_2, x) \in \mathbf{D}_\epsilon$, with $t_1 \leq t_2$. Let us denote by s_1 (respectively s_2) the path length from x to $\mathfrak{C}(t_1, x)$ (respectively $\mathfrak{C}(t_2, x)$) along the trajectory of x and $r_1 = \mathcal{R}(\mathfrak{C}(t_1, x)) - \mathcal{R}(x)$ (respectively $r_2 = \mathcal{R}(\mathfrak{C}(t_2, x)) - \mathcal{R}(x)$). It results from the equalities (3)–(5) and inequation (8) that, along such a trajectory, one has

$$\beta(t_2 - t_1) < (s_2 - s_1) \leq (t_2 - t_1), \quad (9)$$

$$\beta(s_2 - s_1) < (r_2 - r_1) \leq (s_2 - s_1), \quad (10)$$

$$\beta^2(t_2 - t_1) < (r_2 - r_1) \leq (t_2 - t_1). \quad (11)$$

It results from inequalities (11) that \mathfrak{C}_r is Lipschitz in the variable r , because \mathfrak{C} is Lipschitz with respect to the variable t . The lemma below states that \mathfrak{C}_r is also Lipschitz with respect to both variables.

Lemma 3.6. *For any $\epsilon > 0$, using again the β of Lemma 3.5, one has:*

$$\forall x_1, x_2 \in \mathbf{D}_\epsilon, \quad \forall r_1 \in [0, \text{wfs} - \epsilon - \mathcal{R}(x_1)], \quad \forall r_2 \in [0, \text{wfs} - \epsilon - \mathcal{R}(x_2)],$$

$$\|\mathfrak{C}_r(r_2, x_2) - \mathfrak{C}_r(r_1, x_1)\| \leq \frac{1}{\beta} |r_2 - r_1| + \left(\left(1 + \frac{1}{\beta} \right) e^{\frac{\text{wfs}}{\beta^2}} + \frac{1}{\beta} \right) \|x_2 - x_1\|.$$

Proof. With the notation of the lemma, let us call t_1 (respectively t_2) the value in $[0, \frac{\text{wfs}}{\beta^2}]$ such that $\mathfrak{C}_r(r_1, x_1) = \mathfrak{C}(t_1, x_1)$ (respectively $\mathfrak{C}_r(r_2, x_2) = \mathfrak{C}(t_2, x_2)$). Without loss of generality, one can assume that $t_1 \leq t_2$, which ensures that $\mathfrak{C}(t_1, x_2) \in \mathbf{D}_\epsilon$.

The case $\mathcal{R}(x_2) \geq \mathcal{R}(\mathfrak{C}(t_1, x_1))$ is considered later. Therefore, we first assume that $\mathcal{R}(x_2) < \mathcal{R}(\mathfrak{C}(t_1, x_1))$.

In this case, there exists a value t'_1 such that:

$$\mathcal{R}(\mathfrak{C}(t'_1, x_2)) = \mathcal{R}(\mathfrak{C}(t_1, x_1)).$$

One has:

$$\begin{aligned} \mathfrak{C}_r(r_2, x_2) - \mathfrak{C}_r(r_1, x_1) &= \mathfrak{C}(t_2, x_2) - \mathfrak{C}(t_1, x_1) \\ &= \mathfrak{C}(t_2, x_2) - \mathfrak{C}(t'_1, x_2) \\ &\quad + \mathfrak{C}(t'_1, x_2) - \mathfrak{C}(t_1, x_2) \\ &\quad + \mathfrak{C}(t_1, x_2) - \mathfrak{C}(t_1, x_1) \end{aligned}$$

and:

$$\|\mathfrak{C}_r(r_2, x_2) - \mathfrak{C}_r(r_1, x_1)\| \leq \|\mathfrak{C}(t_1, x_2) - \mathfrak{C}(t_1, x_1)\| \quad (12)$$

$$+ \|\mathfrak{C}(t'_1, x_2) - \mathfrak{C}(t_1, x_2)\| \quad (13)$$

$$+ \|\mathfrak{C}(t_2, x_2) - \mathfrak{C}(t'_1, x_2)\|. \quad (14)$$

From Lemma 4.13 in [27], one has:

$$\|\mathfrak{C}(t_1, x_2) - \mathfrak{C}(t_1, x_1)\| \leq e^{\frac{1}{\beta} t_1} \|x_2 - x_1\|$$

and then:

$$\|\mathfrak{C}(t_1, x_2) - \mathfrak{C}(t_1, x_1)\| \leq e^{\frac{1}{\beta^2} \text{wfs}} \|x_2 - x_1\|$$

and that bounds term (12). But we know that the map \mathcal{R} is 1-Lipschitz, which gives:

$$|\mathcal{R}(\mathfrak{C}(t_1, x_2)) - \mathcal{R}(\mathfrak{C}(t_1, x_1))| \leq e^{\frac{1}{\beta^2}} \|x_2 - x_1\|$$

or, using the definition of t'_1 :

$$|\mathcal{R}(\mathfrak{C}(t_1, x_2)) - \mathcal{R}(\mathfrak{C}(t'_1, x_2))| \leq e^{\frac{1}{\beta^2}} \|x_2 - x_1\|.$$

Along the trajectory of x_2 between $\mathfrak{C}(t_1, x_2)$ and $\mathfrak{C}(t'_1, x_2)$, in some increasing order, one can apply inequality (10) which gives:

$$\|\mathfrak{C}(t_1, x_2) - \mathfrak{C}(t'_1, x_2)\| \leq \frac{1}{\beta} e^{\frac{1}{\beta^2}} \|x_2 - x_1\|$$

and that bounds term (13).

In order to bound the third term $\|\mathfrak{C}(t_2, x_2) - \mathfrak{C}(t'_1, x_2)\|$, note that:

$$\begin{aligned} |\mathcal{R}(\mathfrak{C}(t_2, x_2)) - \mathcal{R}(\mathfrak{C}(t'_1, x_2))| &= |\mathcal{R}(\mathfrak{C}(t_2, x_2)) - \mathcal{R}(\mathfrak{C}(t_1, x_1))| \\ &= |\mathcal{R}(x_2) + r_2 - \mathcal{R}(x_1) - r_1| \\ &\leq |\mathcal{R}(x_2) - \mathcal{R}(x_1)| + |r_2 - r_1| \\ &\leq \|x_2 - x_1\| + |r_2 - r_1| \end{aligned}$$

and, along the trajectory of x_2 between $\mathfrak{C}(t_2, x_2)$ and $\mathfrak{C}(t'_1, x_2)$, in some increasing order, one can apply inequality (10)

$$\|\mathfrak{C}(t_2, x_2) - \mathfrak{C}(t'_1, x_2)\| \leq \frac{1}{\beta} (\|x_2 - x_1\| + |r_2 - r_1|)$$

and that bounds the last term.

Let us assume now that:

$$\mathcal{R}(x_2) \geq \mathcal{R}(\mathfrak{C}(t_1, x_1)) = \mathcal{R}(x_1) + r_1.$$

In this case, one has (recall that \mathcal{R} is 1-Lipschitz):

$$r_1 \leq |\mathcal{R}(x_2) - \mathcal{R}(x_1)| \leq \|x_2 - x_1\| \tag{15}$$

and

$$r_2 \leq \|x_2 - x_1\| + |r_2 - r_1|. \tag{16}$$

One has

$$\|\mathfrak{C}_r(r_2, x_2) - \mathfrak{C}_r(r_1, x_1)\| \leq \|\mathfrak{C}(t_2, x_2) - x_2\| + \|x_2 - x_1\| + \|\mathfrak{C}(t_1, x_1) - x_1\|. \tag{17}$$

From inequations (10) one get:

$$\begin{aligned} \|\mathfrak{C}(t_1, x_1) - x_1\| &\leq \frac{r_1}{\beta} \\ \|\mathfrak{C}(t_2, x_2) - x_2\| &\leq \frac{r_2}{\beta} \end{aligned}$$

and, using Eqs. (15) and (16):

$$\begin{aligned} \|\mathfrak{C}(t_1, x_1) - x_1\| &\leq \frac{\|x_2 - x_1\|}{\beta}, \\ \|\mathfrak{C}(t_2, x_2) - x_2\| &\leq \frac{\|x_2 - x_1\| + |r_2 - r_1|}{\beta}. \end{aligned}$$

And (17) gives:

$$\|\mathfrak{C}_r(r_2, x_2) - \mathfrak{C}_r(r_1, x_1)\| \leq \frac{1}{\beta}|r_2 - r_1| + \left(1 + \frac{2}{\beta}\right)\|x_2 - x_1\|. \quad (18)$$

And this is always less than the bound given in the lemma. \square

Remark 3.6.1. Notice that, if $\epsilon_1 < \epsilon_2$, the map \mathfrak{C}_r defined on D_{ϵ_1} extends the map \mathfrak{C}_r defined on D_{ϵ_2} : they coincide on D_{ϵ_2} . Therefore, \mathfrak{C}_r is defined without ambiguity on $\bigcup_{\epsilon>0} D_\epsilon = \mathcal{O} \setminus \overline{\mathcal{O}_{\text{wfs}}}$. \mathfrak{C}_r is locally Lipschitz and therefore continuous.

Following [27], we denote by \mathcal{O}_d the set of points of \mathcal{O} at distance greater than d from the boundary:

$$\mathcal{O}_d = \{x \in \mathcal{O}, \mathcal{R}(x) > d\}$$

and by $\overline{\mathcal{O}_d}$ the closure of \mathcal{O}_d .

Theorem 1. *If $d < \text{wfs}(\mathcal{O})$, $\overline{\mathcal{O}_d}$ is a deformation retract of \mathcal{O} and \mathcal{O}_d has the homotopy type of \mathcal{O} .*

Proof. Proposition 2.2 gives the definition of a deformation retract. Assuming $d < \text{wfs}(\mathcal{O})$, we define the map H_d :

$$\begin{aligned} H_d : [0, 1] \times \mathcal{O} &\mapsto \mathcal{O} \\ (t, x) &\mapsto H_d(t, x) = \begin{cases} \mathfrak{C}_r(t(d - \mathcal{R}(x)), x) & \text{if } \mathcal{R}(x) \leq d, \\ =x & \text{if } \mathcal{R}(x) \geq d. \end{cases} \end{aligned}$$

H_d is a deformation retract of \mathcal{O} toward $\overline{\mathcal{O}_d}$. Let $\epsilon = \frac{\text{wfs} - d}{2}$. The map $H_{d+\epsilon}$ defines the homotopy equivalence of \mathcal{O} toward \mathcal{O}_d using the characterization given in Proposition 2.2. \square

We define $\mathbf{G}_\beta^d(\mathcal{O})$, the smallest superset of $\mathcal{O}_d \cap \mathbf{F}_\beta(\mathcal{O})$ that is globally invariant by the action of $x \mapsto \mathfrak{C}(t, x)$:

$$\begin{aligned} \mathbf{G}_\beta^d(\mathcal{O}) &= \mathfrak{C}(\mathbb{R}^+, \mathcal{O}_d \cap \mathbf{F}_\beta(\mathcal{O})) \\ &= \{x \in \mathcal{O}, \exists t \in \mathbb{R}^+, \exists y \in \mathcal{O}_d \cap \mathbf{F}_\beta(\mathcal{O}), x = \mathfrak{C}(t, y)\}. \end{aligned}$$

Lemma 3.7. *If $d < \text{wfs}(\mathcal{O})$ and $\beta > 0$, \mathbf{G}_β^d has the homotopy type of \mathcal{O} .*

Proof. We use once again the characterization given in Proposition 2.2. One has trivially $\mathbf{G}_\beta^d \subset \overline{\mathcal{O}_d}$. Using Lemma 3.2 one gets the homotopy equivalence with $\overline{\mathcal{O}_d}$ using the homotopy $[0, 1] \times \overline{\mathcal{O}_d} \mapsto \overline{\mathcal{O}_d}$ defined by $(t, x) \mapsto \mathfrak{C}(t(\frac{D}{\beta}), x)$. This together with Theorem 1 gives the result. \square

3.3. Homotopy type of $\mathcal{M}_\lambda(\mathcal{O})$

Lemma 3.8. *If $\lambda < \text{wfs}(\mathcal{O})$, then there exists $\beta > 0$ such that*

$$\mathbf{G}_\beta^\lambda \subset \mathcal{M}_\lambda(\mathcal{O}).$$

Proof. Let us assume that $\lambda < \text{wfs}(\mathcal{O})$, and let us define $\epsilon > 0$ as:

$$\epsilon = \min\left(\frac{\lambda}{2}, \frac{\text{wfs}(\mathcal{O}) - \lambda}{2}\right).$$

From Lemma 3.5 and the definition of $\text{wfs}(\mathcal{O})$, we know that there exists $\beta_0 > 0$ such that:

$$\forall \beta, 0 < \beta \leq \beta_0, d(\mathcal{O}^\circ, \mathcal{O}_\lambda \cap \mathbf{F}_\beta(\mathcal{O})) > \lambda + \epsilon. \quad (19)$$

Let us choose β such that $0 < \beta \leq \beta_0$ and $(\lambda + \epsilon)\sqrt{1 - \beta^2} > \lambda$. Now, if $y \in \mathcal{O}_\lambda \cap \mathbf{F}_\beta(\mathcal{O})$, one has:

$$\begin{aligned} \mathcal{R}(y) &> \lambda + \epsilon \\ \|\nabla(y)\| &\leq \beta \end{aligned}$$

which means, by Eq. (1):

$$\begin{aligned} \mathcal{R}(y) &> \lambda + \epsilon, \\ \sqrt{1 - \frac{\mathcal{F}(y)^2}{\mathcal{R}(y)^2}} &\leq \beta. \end{aligned}$$

Which entails:

$$\mathcal{F}(y) > (\lambda + \epsilon)\sqrt{1 - \beta^2} > \lambda.$$

We have proved so far that $\mathcal{O}_\lambda \cap \mathbf{F}_\beta(\mathcal{O}) \subset \mathcal{M}_\lambda(\mathcal{O})$.

For any point $x \in \mathbf{G}_\beta^\lambda$, there exist $t \in \mathbb{R}^+$ and $y \in \mathcal{O}_\lambda \cap \mathbf{F}_\beta(\mathcal{O})$ such that $x = \mathfrak{C}(t, y)$. Now, recall that the map $t \mapsto \mathcal{F}(\mathfrak{C}(t, x))$ is increasing (see [27]) and therefore $\mathcal{F}(x) \geq \mathcal{F}(y)$. One gets that $\mathcal{F}(x) \geq \mathcal{F}(y) > \lambda$, which entails $x \in \mathcal{M}_\lambda(\mathcal{O})$. \square

Theorem 2. *If $\lambda < \text{wfs}(\mathcal{O})$, $\mathcal{M}_\lambda(\mathcal{O})$ has the homotopy type of \mathcal{O} .*

Proof. We use once again the characterization given in Proposition 2.2. Because the map $t \mapsto \mathcal{F}(\mathfrak{C}(t, x))$ is increasing and from the definition of $\mathcal{M}_\lambda(\mathcal{O})$ it is clear that

$$\forall x \in \mathcal{M}_\lambda(\mathcal{O}), \forall t \in \mathbb{R}^+, \mathfrak{C}(t, x) \in \mathcal{M}_\lambda(\mathcal{O}).$$

With the value of β taken from Lemma 3.8 and using Lemma 3.2 again, one get that the map $[0, 1] \times \mathcal{M}_\lambda(\mathcal{O}) \mapsto \mathcal{M}_\lambda(\mathcal{O})$ defined by $(t, x) \mapsto \mathfrak{C}(t \frac{D}{\beta}, x)$ defines an homotopy equivalence between $\mathcal{M}_\lambda(\mathcal{O})$ and \mathbf{G}_β^d . This, together with Lemma 3.7, proves the theorem. \square

3.4. Weak feature size and singular points of distance functions

The vector field ∇ and the weak feature size are closely related to the critical points of distance functions. Distance functions have been intensively studied (see [26,23] for example) and the aim of this section is to show how properties of such functions apply to our setting. As a consequence, we prove that any bounded open subset with piecewise analytic boundary has a positive weak feature size.

As in previous sections, \mathcal{O} is a bounded open subset of \mathbb{R}^n , $\mathcal{R} : \mathcal{O} \rightarrow \mathbb{R}^+$ is the function defined by $\mathcal{R}(x) = d(x, \mathcal{O}^c)$ and ∇ is the “gradient” of \mathcal{R} as defined in Section 2.1. Recall that a point $x \in \mathcal{O}$ is a singular point of ∇ (i.e., $\nabla(x) = 0$) if and only if it lies in the convex hull of $\Gamma(x)$. So the singular points of ∇ are exactly the singular points of the generalized Clarke gradient of the function \mathcal{R} (see [12,13,23]) that is the singular points of the function \mathcal{R} . The weak feature size is thus the distance between \mathcal{O}^c and the set F of singular points of \mathcal{R} .

In some way the properties of the distance function to a compact set are very similar to the smooth functions ones. In particular, they satisfy an Isotopy Lemma [26], that we reproduce below (Proposition 3.9). Notice that Theorem 1 above could have been proven as a Corollary of Proposition 3.9. We choose to keep our proof. It makes the paper self-contained and preserves the unity of proofs built around the properties of the vector fields ∇ and associated flows \mathfrak{C}_r and \mathfrak{C} . Also, our proof is more detailed and provides an explicit expression of the deformation retract.

Proposition 3.9. *If $0 < \rho_1 < \rho_2$ are such that $\mathbf{F} \cap (\overline{\mathcal{O}}_{\rho_1} \setminus \mathcal{O}_{\rho_2}) = \emptyset$, then all the levels $\mathcal{R}^{-1}(\rho)$, $\rho \in [\rho_1, \rho_2]$, are homeomorphic topological manifolds and*

$$\overline{\mathcal{O}}_{\rho_1} \setminus \mathcal{O}_{\rho_2} = \{x \in \mathcal{O} : \rho_1 \leq \mathcal{R}(x) \leq \rho_2\}$$

is homeomorphic to $\mathcal{R}^{-1}(\rho_1) \times [\rho_1, \rho_2]$. As a consequence, \mathcal{O}_{ρ_1} and \mathcal{O}_{ρ_2} are homotopy equivalent.

As a consequence, if \mathcal{O} has a positive wfs, then for all values $\rho \in]0, \text{wfs}[$, the level sets \mathcal{O}_ρ are homeomorphic topological manifolds, even if the boundary of \mathcal{O} is not a manifold (see Fig. 4).

If $n = 3$, the function \mathcal{R} satisfies a Sard theorem ([23]):

Proposition 3.10. *If $n = 3$, then the set of critical values of \mathcal{R} ,*

$$\text{Crit}(\mathcal{R}) = \mathcal{R}(\mathbf{F}) = \mathcal{R}(\{x \in \mathcal{O} : \nabla(x) = 0\})$$

is a compact set with zero Lebesgue measure in \mathbb{R} .

Note that such a result is false without the hypothesis $n = 3$ (see [23]). Nevertheless, if the open set \mathcal{O} is piecewise analytic (see [10]) one has a stronger result.

Proposition 3.11. *Let \mathcal{O} be a piecewise analytic bounded open set. The set of critical values of \mathcal{R} ,*

$$\text{Crit}(\mathcal{R}) = \mathcal{R}(\mathbf{F}) = \mathcal{R}(\{x \in \mathcal{O} : \nabla(x) = 0\})$$

is finite. In particular $\text{wfs}(\mathcal{O}) > 0$.

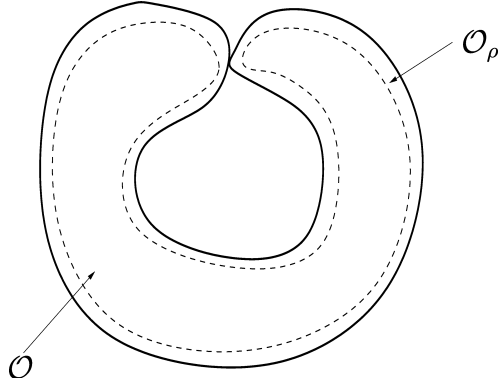


Fig. 4. An open set with positive wfs and nonmanifold boundary.

Proof. This result has been proven by Fu [23, p. 1045] for semialgebraic sets. The proof given here is an immediate adaptation of Fu’s proof based upon stratifiability properties of piecewise analytic sets (see [6,7] or [10]). It is based upon the following lemma due to Ferry [21] (see also [23, p. 1038]). If $x, y \in \mathcal{O}$ are such that $\nabla(x) = \nabla(y) = 0$, then

$$|\mathcal{R}(x) - \mathcal{R}(y)| \leq \frac{1}{2 \min(\mathcal{R}(x), \mathcal{R}(y))} \|x - y\|^2.$$

Note that \mathcal{R} and $\nabla^{-1}(0)$ are subanalytic (see [10]). So there exists a finite analytic stratification of $\nabla^{-1}(0) = M_1 \cup \dots \cup M_k$ such that each M_i is an real analytic manifold and the restriction of \mathcal{R} to M_i is an analytic function. It follows from previous lemma that the derivative of \mathcal{R} restricted to M_i is zero. So \mathcal{R} is constant on M_i . This concludes the proof of proposition. \square

4. Stability of \mathcal{M}_λ under perturbations

The aim of this section is to prove that the λ -medial axis of an open bounded subset of \mathbb{R}^n satisfies some stability properties when one makes a small perturbation of the open set (for Hausdorff distance). Let \mathcal{O} be an open bounded subset of \mathbb{R}^n , let $D = \sup_{(x,y) \in \mathcal{O}} d(x,y)$ be its diameter and let $\lambda > 0$ be a fixed real number.

Theorem 3. *Let $\varepsilon > 0$ be such that $10\varepsilon < \lambda$. For any bounded open set $\tilde{\mathcal{O}}$ such that $d_H(\mathcal{O}^c, \tilde{\mathcal{O}}^c) < \varepsilon$, for any $x \in \mathcal{M}_\lambda(\tilde{\mathcal{O}})$ and for any $\lambda' > 0$ such that $\lambda'^2 < \lambda^2 - 150\sqrt{\varepsilon}D^{3/2}$ and $\lambda' < \lambda - \varepsilon$, there exists a point $y \in \mathcal{M}_{\lambda'}(\mathcal{O})$ such that*

$$d(x,y) \leq 2\sqrt{D}\sqrt{\varepsilon}.$$

Note that the result makes sense only if ε is small enough, i.e., it satisfies $150\sqrt{\varepsilon}D^{3/2} < \lambda^2$. The idea of the proof of this theorem is to show that if $y(s)$ is the trajectory of the vector field ∇ issued from x , then it cannot remain during a long time outside of some $\mathcal{M}_{\lambda'}(\mathcal{O})$ for a well chosen value of λ' .

Proof. From now on, one fixes a real $\varepsilon > 0$ and an open set $\tilde{\mathcal{O}}$ satisfying the hypothesis of the theorem. The notations $\tilde{\mathcal{R}}, \tilde{\mathcal{F}}, \tilde{\nabla}$ will, respectively, denote the distance function, the minimum radius function, and the “gradient” vector field associated to $\tilde{\mathcal{O}}$. Since $\lambda > 2\varepsilon$, one has $\mathcal{M}_\lambda(\tilde{\mathcal{O}}) \subset \mathcal{O}$ and $\mathcal{M}_\lambda(\mathcal{O}) \subset \tilde{\mathcal{O}}$. Let $x \in \mathcal{M}_\lambda(\tilde{\mathcal{O}})$. The ball $\mathbb{B}_{x, \mathcal{R}(x)}$ of radius $\mathcal{R}(x) > 0$ and center x does not contain any point of $\partial\mathcal{O}$ in its interior. Because $d_{\text{H}}(\mathcal{O}^c, \tilde{\mathcal{O}}^c) < \varepsilon$, the ball $\mathbb{B}_{x, \mathcal{R}(x)-\varepsilon}$ does not intersect the boundary $\partial\tilde{\mathcal{O}}$ of $\tilde{\mathcal{O}}$. So, $\mathcal{R}(x) - \varepsilon \leq \tilde{\mathcal{R}}(x)$. In the same way, the sphere of center x and radius $\mathcal{R}(x)$ contains some point of $\partial\mathcal{O}$, so the ball $\mathbb{B}_{x, \mathcal{R}(x)+\varepsilon}$ contains some point of $\partial\tilde{\mathcal{O}}$ and then $\tilde{\mathcal{R}}(x) \leq \mathcal{R}(x) + \varepsilon$. We thus have proved

$$\mathcal{R}(x) - \varepsilon \leq \tilde{\mathcal{R}}(x) \leq \mathcal{R}(x) + \varepsilon. \quad (20)$$

An immediate consequence of these inequalities and $\tilde{\mathcal{R}}(x) \geq \lambda$ is that $\mathcal{R}(x) \geq \lambda - \varepsilon$. It follows that if $\nabla(x) = 0$, then $\mathcal{R}(x) = \mathcal{F}(x) \geq \lambda - \varepsilon$ and x belongs to $\mathcal{M}_{\lambda'}(\mathcal{O})$ for any $\lambda' < \lambda - \varepsilon$. From now on, suppose $\nabla(x) \neq 0$ and let $y(s)$ be the “trajectory” of point x for vector field ∇ parametrized by arc-length and such that $y(0) = x$. While this trajectory remains in the complementary of $\mathcal{M}_{\lambda'}(\mathcal{O})$ for some $\lambda' < \lambda - \varepsilon$, one has

$$\frac{d\mathcal{R}}{ds}(y(s)) = \|\nabla(y(s))\| \geq \sqrt{1 - \frac{\lambda'^2}{\mathcal{R}(y(s))^2}}.$$

Thus using the fact that $\mathcal{R}(\cdot)$ is increasing along trajectories of ∇ it follows

$$\mathcal{R}(y(s)) \frac{d\mathcal{R}}{ds}(y(s)) = \frac{1}{2} \frac{d\mathcal{R}^2}{ds}(y(s)) \geq \sqrt{\mathcal{R}^2(y(s)) - \lambda'^2} \geq \sqrt{\mathcal{R}^2(x) - \lambda'^2}$$

which implies

$$\mathcal{R}^2(x) + 2s\sqrt{\mathcal{R}^2(x) - \lambda'^2} \leq \mathcal{R}^2(y(s)). \quad (21)$$

Denote by

$$\tilde{\Gamma}(x) = \{y \in \tilde{\mathcal{O}}^c : d(x, y) = d(x, \tilde{\mathcal{O}}^c)\} \subset \tilde{\mathcal{O}}^c$$

the set of closest boundary points and denote by \tilde{B} the smallest ball containing this set. Its radius is equal to $\tilde{\mathcal{F}}(x) \geq \lambda$. Let C be the cone of apex x constructed on the $(n-2)$ -sphere $\tilde{S} = \mathbb{S}_{x, \tilde{\mathcal{R}}(x)} \cap \partial\tilde{B}$ and let $2\alpha_1$ be its apex angle (see Fig. 5).

Lemma 4.1.

Angle α_1 satisfies the following inequation

$$2(\mathcal{R}(x) - \varepsilon)^2 \cos(2\alpha_1) = 2(\mathcal{R}(x) - \varepsilon)^2(2\cos^2\alpha_1 - 1) \leq 2(\mathcal{R}(x) + \varepsilon)^2 - 4\lambda^2. \quad (22)$$

Proof. Recall from [27], that the $(n-2)$ -sphere \tilde{S} is of radius $\tilde{\mathcal{F}}(x)$ and contains $\tilde{\Gamma}(x)$. Let p, q be two points such that segment $[pq]$ is a diameter of this $(n-2)$ -sphere (see Fig. 5). These points satisfy $d(x, p) = d(x, q) = \tilde{\mathcal{R}}(x)$ and since $x \in \mathcal{M}_\lambda(\tilde{\mathcal{O}})$, $d(p, q) \geq 2\lambda$. It follows from inequality (20) that $\mathcal{R}(x) - \varepsilon \leq d(x, p) = d(x, q) \leq \mathcal{R}(x) + \varepsilon$. Lemma’s inequality is thus an immediate consequence of the classical relation between edges of the triangle (x, p, q)

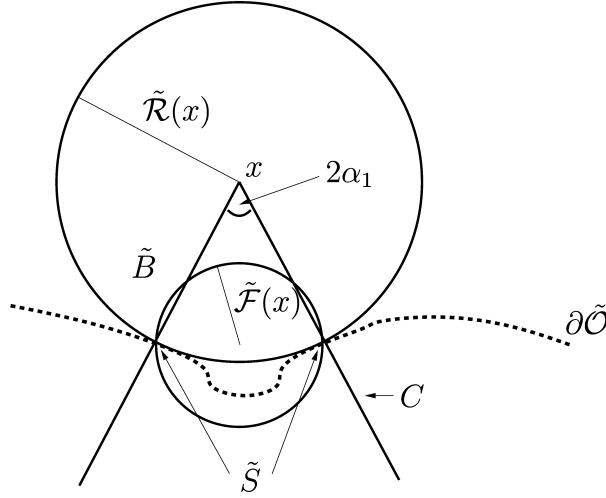


Fig. 5. The small circle depicts the smallest ball containing the set of closest boundary points.

$$2 \cos(2\alpha_1) d(x, p) \cdot d(x, q) = d(x, p)^2 + d(x, q)^2 - d(p, q)^2. \quad \square$$

Lemma 4.2. *The distance $\mathcal{R}(y(s))$ between $y(s)$ and $\partial\mathcal{O}$ satisfies*

$$\mathcal{R}(y(s))^2 \leq \left(\varepsilon + \sqrt{(\mathcal{R}(x) + \varepsilon)^2 + s^2 + 2s(\mathcal{R}(x) + \varepsilon) \cos \alpha_1} \right)^2. \quad (23)$$

Proof. Distance between \mathcal{O}^c and $\tilde{\mathcal{O}}^c$ being less than ε , $\mathcal{R}(y(s))$ must satisfy $\mathcal{R}^2(y(s)) \leq (\tilde{\mathcal{R}}(y(s)) + \varepsilon)^2$. Since $y(s)$ is parametrized by arc-length, it follows from Lemma 4.15 in [27] applied to functions $\tilde{\mathcal{R}}$ and $\tilde{\mathcal{F}}$ in $\tilde{\mathcal{O}}$ that

$$\tilde{\mathcal{R}}(y(s)) \leq \sqrt{\tilde{\mathcal{R}}(x)^2 + 2s\sqrt{\tilde{\mathcal{R}}(x)^2 - \tilde{\mathcal{F}}(x)^2} + s^2}.$$

Using that $\tilde{\mathcal{R}}(x)^2 - \tilde{\mathcal{F}}(x)^2 = \tilde{\mathcal{R}}(x)^2(1 - \sin^2(\alpha_1))$ and that $\tilde{\mathcal{R}}(x) \leq \mathcal{R}(x) + \varepsilon$ one deduces immediately the requested inequality. \square

The end of the proof of Theorem 3 will now follow from computations using inequalities (21)–(23). Eq. (21) forces $\mathcal{R}(y(s))$ to increase sufficiently fast while Eq. (23) forces increasing of $\mathcal{R}(y(s))$ to be sufficiently slow. The computations below show that these two conditions cannot be simultaneously satisfied for a large range of values of s . In order to simplify notations, introduce the following notations

$$E = \frac{\varepsilon}{\mathcal{R}(x)}, \quad S = \frac{s}{\mathcal{R}(x)}, \quad A = \frac{\lambda}{\mathcal{R}(x)}, \quad A' = \frac{\lambda'}{\mathcal{R}(x)}.$$

Inequalities (21) and (23) lead to

$$1 + 2S\sqrt{1 - A'^2} \leq \left(E + \sqrt{(1 + E)^2 + S^2 + 2S(1 + E) \cos \alpha_1} \right)^2$$

which is equivalent to

$$1 + 2S\sqrt{1 - A^2} \leq E^2 + (1 + E)^2 + S^2 + 2S(1 + E) \cos \alpha_1 \\ + 2E\sqrt{(1 + E)^2 + S^2 + 2S(1 + E) \cos \alpha_1}$$

and which becomes (using that $\sqrt{1 + u} \leq 1 + u/2$ for all $u \geq 0$),

$$2S\sqrt{1 - A^2} \leq (4E + 4E^2 + E^3) + 2S(1 + E)^2 \cos \alpha_1 + (1 + E)S^2.$$

Now, Eq. (22) is equivalent to

$$2\cos^2 \alpha_1 \leq 1 + \frac{(1 + E)^2}{(1 - E)^2} - \frac{2A^2}{(1 - E)^2}.$$

Using that $(1 + E)^2 = (1 - E)^2 + 4E$ one deduces that

$$\cos^2 \alpha_1 \leq 1 + \frac{2E}{(1 - E)^2} - \frac{A^2}{(1 - E)^2}.$$

Recall that $\varepsilon < \lambda/10$ and $\mathcal{R}(x) \geq \lambda - \varepsilon$, which entails that $E < 1/9$. In particular, one has $1/2 < (1 - E)^2 \leq 1$. With this, previous inequation implies

$$\cos^2 \alpha_1 \leq 1 + \frac{2E}{(1 - E)^2} - \frac{A^2}{(1 - E)^2} \leq 1 + 4E - A^2$$

and using that $E < 1$, one obtains

$$9E + 2SA + (1 + E)S^2 \geq 0, \quad A = \left((1 + E)^2 \sqrt{1 + 4E - A^2} - \sqrt{1 - A^2} \right). \quad (24)$$

Claim 1.

Choosing $A^2 < A^2 - 150\sqrt{E}$ (i.e., $\lambda^2 < \lambda^2 - 150\mathcal{R}^{3/2}(x)\sqrt{\varepsilon}$), one has $A < -5\sqrt{E}$.

Proof. Note that condition $A < -5\sqrt{E}$ is equivalent to

$$1 - A^2 > (1 + 2E + E^2)^2(1 + 4E - A^2) + 25E + 10\sqrt{E}(1 + E)^2\sqrt{1 + 4E - A^2}.$$

Remark that $A^2(1 + 2E + E^2)^2 > A^2$ and, since $E < 1/8$, one has $(1 + 2E + E^2)^2(1 + 4E) - 1 < 12E$. Thus previous condition is implied by

$$A^2 < A^2 - 12E - 25E - 10\sqrt{E}(1 + E)^2\sqrt{1 + 4E - A^2}.$$

Now, using that $10\sqrt{E}(1 + E)\sqrt{1 + 4E - A^2} < 100\sqrt{E}$, this last condition is implied by

$$A^2 < A^2 - 37E - 100\sqrt{E}$$

which is implied by

$$A'^2 < A^2 - 150\sqrt{E}. \quad \square$$

It follows from previous claim that the discriminant of inequation (24) satisfies

$$A' = A^2 - 9E(1 + E) > 7E > 0$$

which implies that the inequation is not satisfied for

$$S \in \left[\frac{-A - \sqrt{A'}}{1 + E}, \frac{-A + \sqrt{A'}}{1 + E} \right].$$

So the trajectory $y(s)$ cannot remain in \mathcal{M}_{λ^c} for $S = \frac{-A - \sqrt{A'}}{1 + E} > 0$. Now, using that $\sqrt{1 - u} \geq 1 - u$ for all $u \in [0, 1]$, it comes

$$-A - \sqrt{A'} = -A \left(1 - \sqrt{1 - \frac{9E(1 + E)}{A^2}} \right) \leq -\frac{9E(1 + E)}{A}.$$

Since $-A > 5\sqrt{E}$, it follows that

$$\frac{-A - \sqrt{A'}}{1 + E} < \frac{9\sqrt{E}}{5}$$

which implies that $y(s)$ cannot remain in \mathcal{M}_{λ^c} for $S \geq 2\sqrt{E}$, i.e., for $s > 2\sqrt{\mathcal{R}(x)\varepsilon}$. We thus have proved Theorem 3. \square

In case one wants to estimate the distance of $\mathcal{M}_{\lambda}(\tilde{\mathcal{O}})$ to the medial axis $\mathcal{M}(\mathcal{O})$ of \mathcal{O} one can deduce a better bound from previous proof.

Corollary 4. *Let $\varepsilon > 0$ such that $\varepsilon < \min(\frac{\lambda}{10}, \frac{\lambda^3}{50D^2}, \frac{\lambda^4}{1200D^4})$. For any bounded open set $\tilde{\mathcal{O}}$ such that $d_{\text{H}}(\mathcal{O}^c, \tilde{\mathcal{O}}^c) < \varepsilon$, for any $x \in \mathcal{M}_{\lambda}(\tilde{\mathcal{O}})$ there exists a point $y \in \mathcal{M}(\mathcal{O})$ such that*

$$d(x, y) \leq \frac{72D^2}{\lambda^2} \varepsilon.$$

Proof. Using notations of above proof, while $y(s)$ remains in the complementary of the closure of the medial axis of \mathcal{O} , inequation (21) becomes

$$\mathcal{R}^2(x) + 2s\mathcal{R}(x) \leq \mathcal{R}^2(y(s)). \quad (25)$$

The same computations as above then lead to

$$9E + 2SA + (1 + E)S^2 \geq 0, \quad A = \left((1 + E)^2 \sqrt{1 + 4E - A^2} - 1 \right). \quad (26)$$

Claim 2.

Let $\beta = \frac{\lambda^2}{8D^2}$. One has $A < -\beta$.

Proof. This is just a computation. The condition $A < -\beta$ is equivalent to

$$A^2 > 1 + 4E - \frac{(1 - \beta)^2}{(1 + E)^4}.$$

Using that $A^2 = \lambda^2/\mathcal{R}^2(x) > \lambda^2/D^2$, this condition is implied by

$$\frac{\lambda^2}{D^2} > 1 + 4E - \frac{(1-\beta)^2}{(1+E)^4} \quad \text{that is} \quad \frac{(1-\beta)^2}{(1+E)^4} > 1 - \frac{\lambda^2}{D^2} + 4E.$$

Since $\lambda \leq \mathcal{R}(x) + \varepsilon$ and $\varepsilon < \lambda^3/(16D^2)$ one has $4E < \frac{\lambda^2}{2D^2}$ and previous condition is thus implied by

$$(1-\beta)^2 > (1+E)^4(1-4\beta) \quad \text{that is} \quad \beta < 1 - (1+E)^2\sqrt{1-4\beta}.$$

Using that $\sqrt{1-u} \leq 1-u/2$ for $u \geq 0$, this last condition is implied by

$$\beta < 1 + (1+E)^2(-1+2\beta) \quad \text{that is} \quad \beta < 2\beta(1+E)^2 - 3E$$

which is clearly satisfied because $\varepsilon < \frac{\lambda^3}{50D^2}$ implies $3E < \beta$. \square

One concludes the proof of corollary in the same way as in the proof of theorem:

$$A' = A^2 - 9E(1+E) > 0 \quad \text{because} \quad \varepsilon < \frac{\lambda^4}{1200D^4}$$

$$\text{and} \quad \frac{-A - \sqrt{A'}}{1+E} \leq -\frac{9E}{A} < \frac{72D^2}{\lambda^2}E.$$

So $y(s)$ cannot remain in the complementary of the closure of $\mathcal{M}(\mathcal{O})$ for $S > \frac{72D^2}{\lambda^2}E$, i.e., for $s > \frac{72D^2}{\lambda^2}\varepsilon$. \square

5. Approximation of λ -medial axis from a noisy sample of points

Results of previous section lead to an algorithm to approximate the λ -medial axis of an open set \mathcal{O} from the Voronoi diagram of a set of points sampled on the boundary of \mathcal{O} . The main interest of this algorithm is twofold. First, no hypothesis on the smoothness of the boundary of \mathcal{O} is needed. Second, noisy samples are allowed, i.e., it is only required that the Hausdorff distance between $\partial\mathcal{O}$ and the sample is bounded by ε .

5.1. Computation of the λ -medial axis of a sample of points

Let \mathcal{O} be a bounded open subset of \mathbb{R}^n which boundary is denoted by $S = \partial\mathcal{O} = \mathcal{O}^c \cap \overline{\mathcal{O}}$.

Definition 5.1. A finite sample of points \mathcal{E} such that the Hausdorff distance between S and \mathcal{E} is less than ε is called an ε -noisy sample of S .

Let \mathcal{E} be an ε -noisy sample and let $\tilde{\mathcal{O}}$ be the open set which is the complementary of \mathcal{E} intersected with $\mathcal{O}^{+\varepsilon} = \{x \in \mathbb{R}^n : d(x, \mathcal{O}) < \varepsilon\}$ (see Fig. 6). Remark that $d_H(\mathcal{O}^c, \tilde{\mathcal{O}}^c) < \varepsilon$.

Lemma 5.2. If $\lambda > \varepsilon$, $\mathcal{M}_\lambda(\tilde{\mathcal{O}})$ is contained in the Voronoi diagram of \mathcal{E} .

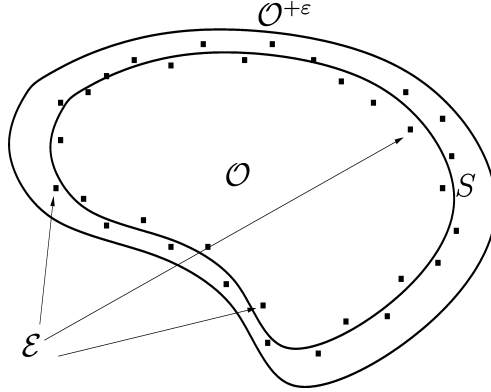


Fig. 6. An ε -noisy sample of S .

Proof. Let $x \in \mathcal{M}_\lambda(\tilde{\mathcal{O}})$ and suppose there exists $z \in (\mathcal{O}^{+\varepsilon})^c$ such that $d(x, z) = \tilde{\mathcal{R}}(x) > \varepsilon$. Thus the ball $\mathbb{B}_{x, \tilde{\mathcal{R}}(x)}$ is contained in $\mathcal{O}^{+\varepsilon}$ and does not contain any point of \mathcal{E} . Points x and z being in \mathcal{O} and $(\mathcal{O}^{+\varepsilon})^c$, respectively, there exists a point y on the segment $[x, z]$ such that $y \in \partial\mathcal{O}$. The ball $\mathbb{B}_{y, \varepsilon}$ does not intersect \mathcal{O} , so $d(y, z) \geq \varepsilon$ which entails $\mathbb{B}_{y, \varepsilon} \subset \mathbb{B}_{x, \tilde{\mathcal{R}}(x)}$. But $\mathbb{B}_{x, \tilde{\mathcal{R}}(x)} \cap \mathcal{E} = \emptyset$ and $d(y, \mathcal{E}) < \varepsilon$ because $d_H(\partial\mathcal{O}, \mathcal{E}) < \varepsilon$, which is a contradiction. Thus one has $\tilde{\Gamma}(x) \subset \mathcal{E}$. This concludes the proof. \square

In the following $\mathcal{M}_\lambda(\tilde{\mathcal{O}})$ will be denoted $\mathcal{M}_\lambda(\mathcal{E})$ and one supposes that $\lambda > \varepsilon$. The “minimum radius function” \mathcal{F}' associated to the open set $\mathbb{R}^n \setminus \mathcal{E}$ is constant on each cell of the Voronoi diagram of \mathcal{E} . It follows from previous lemma that $\mathcal{M}_\lambda(\mathcal{E})$ is the union of the cells of the Voronoi diagram of \mathcal{E} on which \mathcal{F}' is greater or equal to λ . So the following algorithm compute $\mathcal{M}_\lambda(\mathcal{E})$.

- $\mathcal{M}_\lambda(\mathcal{E}) = \emptyset$
- Compute Delaunay triangulation \mathcal{D} of \mathcal{E}
- For each cell c of \mathcal{D} do
 - if c has smallest enclosing ball of radius greater than λ then
 - $\mathcal{M}_\lambda(\mathcal{E}) = \mathcal{M}_\lambda(\mathcal{E}) \cup \text{dual}(c)$.

The algorithm is illustrated in Fig. 7 where one considers a 2D open set bounded by two half-circles of radius 1 and 2 and two segments. The first and the second pictures show the output of the algorithm for noisy samples ($\varepsilon = 0.02$) and values of λ equal to 0.15 (left picture) and 0.2 (right picture). The third picture show the output for a sample without noise and $\lambda = 0.2$.

5.2. Convergence of λ -medial axis

In order to be useful, previous algorithm needs some convergence guarantees. That is one needs to know if the λ -medial axis of an ε -noisy sample of S converges to the λ -medial axis of \mathcal{O} when ε goes to 0 (for the Hausdorff distance). This is not

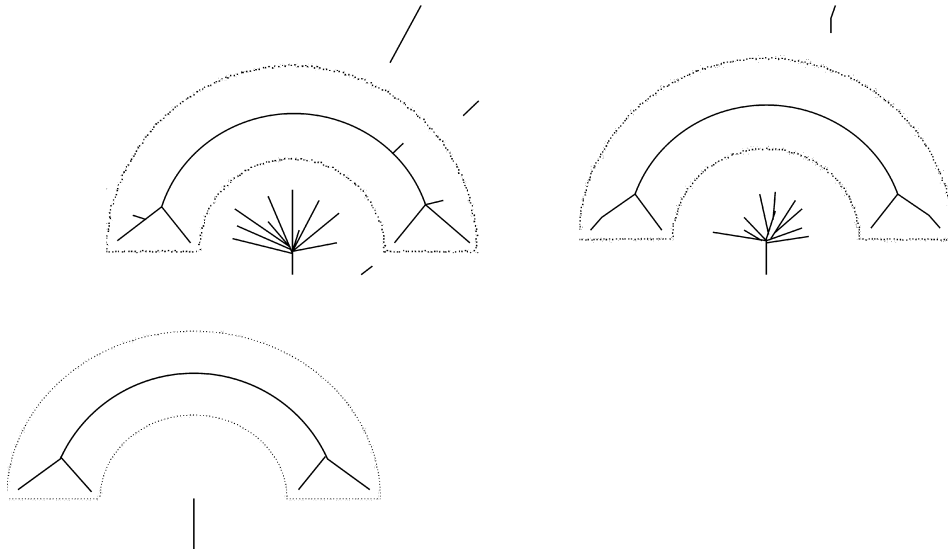


Fig. 7. Examples of approximations of \mathcal{M}_λ for a half-annulus: the two upper ones correspond to noisy inputs ($\varepsilon = 0.02$) $\lambda = 0.15$ (left) and $\lambda = 0.2$ (right). The lower one correspond to exact inputs and $\lambda = 0.2$.

always the case for some values of λ as it is shown in the next example. Consider a cylinder C in \mathbb{R}^3 of radius $\lambda > 0$ and axis (Oz) bounding an open set \mathcal{O} . Then $\mathcal{M}_\lambda(\mathcal{O})$ is exactly the axis of C . But for any $\varepsilon > 0$, if one chooses a ε -noisy sample \mathcal{E} of C on the cylinder of axis (Oz) and radius $\lambda - \varepsilon/2$, then $\mathcal{M}_\lambda(\mathcal{E}) = \emptyset$ (see Fig. 8).

In some sense, such an example and such a value of λ are not “generic.” The lack of convergence is due to the fact that \mathcal{F} is equal to λ on a “big part” of the medial axis of \mathcal{O} , i.e., \mathcal{F} is constant equal to λ on an open subset of $\mathcal{M}(\mathcal{O})$ for the induced

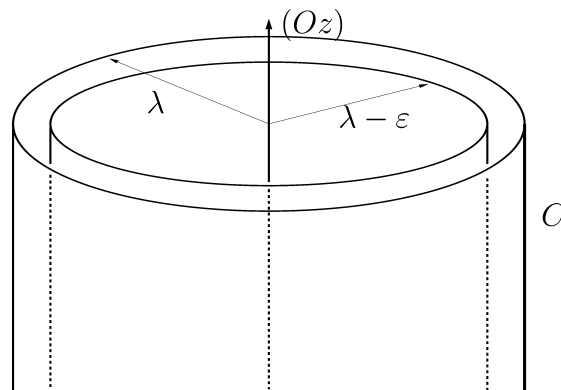


Fig. 8. The λ -medial is unstable on a cylinder of radius λ .

topology on $\mathcal{M}(\mathcal{O})$. Recall from [27] that map \mathcal{F} is upper semicontinuous and then since \mathcal{O} is bounded, $\mathcal{M}_\lambda(\tilde{\mathcal{O}})$ is a compact set for any $\lambda > 0$. Let \mathcal{M} be the map from $]0; +\infty[$ to the set of compact subsets of \mathcal{O} endowed with the topology induced by Hausdorff distance between compact sets (see Section 2.3) defined by $\mathcal{M}(\lambda) = \mathcal{M}_\lambda(\mathcal{O})$. Since \mathcal{F} is upper continuous and since $\mathcal{M}(\lambda) \subseteq \mathcal{M}(\lambda')$ whenever $\lambda' < \lambda$, the map \mathcal{M} is left continuous. This means that if λ_n is an increasing sequence which converges to some $\lambda > 0$, then $d_H(\mathcal{M}_{\lambda_n}(\mathcal{O}), \mathcal{M}_\lambda(\mathcal{O})) \rightarrow 0$ as $n \rightarrow \infty$. The map \mathcal{M} is continuous at λ if previous property is true for any sequence λ_n . Note that in above example \mathcal{M} was not continuous at λ .

Theorem 5. *Let \mathcal{O} be an open bounded subset of \mathbb{R}^n with boundary S and let $\lambda > 0$ be such that the above defined map \mathcal{M} is continuous at λ . For any sequence \mathcal{E}_n of ε_n -noisy samples of S satisfying $\lim_{n \rightarrow +\infty} \varepsilon_n = 0$ one has*

$$d_H(\mathcal{M}_\lambda(\mathcal{E}_n), \mathcal{M}_\lambda(\mathcal{O})) \rightarrow 0 \quad \text{as } n \rightarrow +\infty.$$

Proof. This is a consequence of Theorem 3 and of some classical properties of Hausdorff topology on the set of compact sets in \mathbb{R}^n (see Section 2.3). Let $\varepsilon > 0$ and let \mathcal{E} be a ε -noisy sample of S . It follows from Theorem 3, applied to \mathcal{O} and $\tilde{\mathcal{O}}_\varepsilon = \mathcal{O}^{+\varepsilon} \setminus \mathcal{E}$ symmetrically, that there exist some functions $f(\varepsilon)$, $g_1(\varepsilon)$, and $g_2(\varepsilon)$ such that $\lim_{\varepsilon \rightarrow 0} f(\varepsilon) = \lim_{\varepsilon \rightarrow 0} g_1(\varepsilon) = \lim_{\varepsilon \rightarrow 0} g_2(\varepsilon) = 0$ and such that

$$\mathcal{M}_\lambda(\tilde{\mathcal{O}}_\varepsilon) \subset \mathcal{M}_{\lambda-g_1(\varepsilon)}^{f(\varepsilon)}(\mathcal{O}) = \{x \in \mathbb{R}^n : d(x, \mathcal{M}_{\lambda-g_1(\varepsilon)}(\mathcal{O})) < f(\varepsilon)\}$$

and

$$\mathcal{M}_{\lambda+g_2(\varepsilon)}(\mathcal{O}) \subset \mathcal{M}_\lambda(\tilde{\mathcal{O}}_\varepsilon)^{f(\varepsilon)} = \{x \in \mathbb{R}^n : d(x, \mathcal{M}_\lambda(\tilde{\mathcal{O}}_\varepsilon)) < f(\varepsilon)\}.$$

So,

$$\mathcal{M}_{\lambda+g_2(\varepsilon)}(\mathcal{O}) \subset \mathcal{M}_\lambda(\tilde{\mathcal{O}}_\varepsilon)^{f(\varepsilon)} \subset \mathcal{M}_{\lambda-g_1(\varepsilon)}^{2f(\varepsilon)}(\mathcal{O}).$$

Since \mathcal{M} is continuous at λ ,

$$\lim_{\varepsilon \rightarrow 0} \mathcal{M}_{\lambda+g_2(\varepsilon)}(\mathcal{O}) = \lim_{\varepsilon \rightarrow 0} \mathcal{M}_{\lambda-g_1(\varepsilon)}^{2f(\varepsilon)}(\mathcal{O}) = \mathcal{M}_\lambda(\mathcal{O})$$

which implies Theorem 5. \square

5.3. Genericity of hypothesis of Theorem 5

As mentioned above, the map \mathcal{M} is not always continuous on the whole interval $]0, +\infty[$. Nevertheless under some quite general hypothesis, the number of values λ for which \mathcal{M} is not continuous is finite. Such an hypothesis is in particular satisfied for open sets bounded by piecewise linear manifolds and more generally by piecewise analytic manifolds, such as for example BRep solid.

A precise mathematical definition of piecewise analytic open set in terms of sub-analytic geometry is given in [10]. Roughly speaking, a relatively compact piecewise analytic (or equivalently a subanalytic) set in \mathbb{R}^n is the linear projection of a set which

is defined by analytic equations and inequations in some \mathbb{R}^{n+k} . Such a set may be decomposed into a finite union of smooth analytic manifolds. Note that the boundary of a piecewise analytic set is also piecewise analytic. It is proven in [10] that if \mathcal{O} is a piecewise analytic bounded open set in \mathbb{R}^n , then its medial axis is piecewise analytic. In the same way, $\mathcal{M}_\lambda(\mathcal{O})$ is also piecewise analytic.

Theorem 6. *Let \mathcal{O} be a bounded piecewise analytic open subset of \mathbb{R}^n . There is only a finite number of values $\lambda_1, \dots, \lambda_k$ such that the function \mathcal{M} is not continuous at λ_i , $i = 1, \dots, k$.*

In other words, if $\lambda > 0$ is such that $\lambda \neq \lambda_i$ for all $i = 1, \dots, k$, then $\mathcal{M}_\lambda(\mathcal{O})$ is well approximated by the λ -medial axis of ε -noisy samples $S = \partial\mathcal{O}$.

Proof. The theorem will follow from the fact that the sets $\mathcal{M}_\lambda(\mathcal{O})$ are piecewise analytic and that the function \mathcal{F} restricted to $\mathcal{M}(\mathcal{O})$ is piecewise analytic. This quite technical fact, which is a variant of a result proven in [10], is proven in Lemma A.1. Let $\lambda > 0$ be such that \mathcal{M} is not continuous at λ . Since \mathcal{M} is left continuous, \mathcal{M} is not right continuous at λ . There exists a decreasing sequence (λ_n) which converges to λ such that $d_H(\mathcal{M}_{\lambda_n}(\mathcal{O}), \mathcal{M}_\lambda(\mathcal{O})) \rightarrow 0$ when $n \rightarrow \infty$. The sequence (λ_n) being decreasing, one has $\mathcal{M}_{\lambda_n}(\mathcal{O}) \subseteq \mathcal{M}_{\lambda_{n+1}}(\mathcal{O}) \subseteq \dots \subseteq \mathcal{M}_\lambda(\mathcal{O})$ and there exists $c > 0$ such that $d_H(\mathcal{M}_{\lambda_n}(\mathcal{O}), \mathcal{M}_\lambda(\mathcal{O})) > c$ for any $n > 0$. It follows that there exists an open ball of radius $c/2$ in \mathcal{O} with center on \mathcal{M}_λ which does not intersect any of the $\mathcal{M}_{\lambda'}$, $\lambda' > \lambda$. So if one considers the topology induced on $\mathcal{M}(\mathcal{O})$ by the usual topology on \mathbb{R}^n , the function \mathcal{F} is constant equal to λ on some nonempty open subset of $\mathcal{M}(\mathcal{O})$. Now, $\mathcal{M}(\mathcal{O})$ and \mathcal{F} being piecewise analytic, there exists a finite partition $\mathcal{M}_1, \dots, \mathcal{M}_l$ of $\mathcal{M}(\mathcal{O})$ such that each \mathcal{M}_i is a connected analytic manifold and the restriction of \mathcal{F} to \mathcal{M}_i is an analytic function. So, there exists $i \in \{1, \dots, l\}$ such that the restriction of \mathcal{F} to \mathcal{M}_i is constant equal to λ on some nonempty open subset of \mathcal{M}_i . It follows from a classical property of analytic functions on a connected manifold that \mathcal{F} has to be constant on \mathcal{M}_i . So the number of values λ such that \mathcal{M} is not continuous at λ is less than l . \square

Remark 5.2.1. In practice, one does not know the “bad” values $\lambda_1, \dots, \lambda_k$. In order to take care about them one can use the following heuristic. From a noisy sample of point \mathcal{E} , one can easily compute $\mathcal{M}_{\lambda-\varepsilon}(\mathcal{E})$ and $\mathcal{M}_{\lambda+\varepsilon}(\mathcal{E})$ for some small value $\varepsilon > 0$. If the distance between these two sets is “small enough” one considers that λ is a regular value. Note that it follows from Section 5.1 that such computations need only one computation of the Voronoi diagram of \mathcal{E} .

6. Conclusion

This paper focuses on the properties of the λ -medial axis of an arbitrary bounded open subset of \mathbb{R}^n . Our detailed proofs of these properties make use of the recently introduced [27] vector field ∇ and its corresponding flow \mathfrak{C} .

The stability of the λ -medial axis under Hausdorff distance perturbation of the object boundary (Theorems 3 and 5) makes it computable in practice. Therefore, the λ -medial axis being a more constructive object, is given more “reality” than the “exact” medial axis. The relevance of the λ -medial axis for the question of the computation of medial axes is pointed out by Attali et al. [4].

Beside the stability properties, the new notion of *Weak Feature Size* and the associated theorems on the homotopy type of erosions or λ -medial axes (Theorems 1 and 2) provide us with tools for capturing the homotopy type of a set from a given Hausdorff approximation of its boundary. The smoothness assumption $\text{lfs} > 0$ can now be replaced by the much weaker condition $\text{wfs} > 0$. This line of research has since been followed in [11].

Appendix A. Subanalyticity of \mathcal{F} and $\mathcal{M}_\lambda(\mathcal{O})$

This appendix contains the proof of some result used in above section: the function \mathcal{F} and the λ -medial axis of a piecewise analytic open set are piecewise analytic. Recall that a subset of \mathbb{R}^n is said to be piecewise analytic if it is a subanalytic subset of \mathbb{R}^n . These proofs are classical in the context of subanalytic geometry. The reader may refer to appendix of [10] for a quick introduction to the subject and to [6,7] or [28] for a general introduction. Let $\mathcal{O} \subset \mathbb{R}^n$ be a piecewise analytic bounded open set with boundary S . Note that the function \mathcal{F} is in fact defined for any point $x \in \mathbb{R}^n$ in the same way as for points of \mathcal{O} . It is constant equal to 0 on the complementary of \mathcal{O} . Recall that function \mathcal{F} is said to be subanalytic (or equivalently piecewise analytic) if its graph

$$F = \{(x, t) \in \mathbb{R}^n \times [0, +\infty[: t = \mathcal{F}(x)\}$$

is a subanalytic subset of $\mathbb{R}^n \times [0, +\infty[$.

Lemma A.1. *The function \mathcal{F} is subanalytic, and $\mathcal{M}_\lambda(\mathcal{O})$ is a subanalytic set for any $\lambda > 0$.*

Proof. The proof is very similar to the proof of the subanalyticity of the medial axis given in [10] and is based upon very classical technics in the setting of subanalytic geometry. It is sufficient to prove that \mathcal{F} is subanalytic since $\mathcal{M}_\lambda(\mathcal{O}) = \{x \in \mathcal{O} : \mathcal{F}(x) \geq \lambda\}$ is the canonical linear projection on \mathbb{R}^n of the intersection of the graph F with the half space $\{(x, t) \in \mathbb{R}^n \times [0, +\infty[: t \geq \lambda\}$. Since $S = \partial\mathcal{O}$ is subanalytic, the set

$$A = \{(x, z) \in \mathbb{R}^n \times S : d(x, z) = d(x, S)\}$$

is clearly subanalytic. Remark that $(x, t) \in F$ if and only if

$$(\exists y \text{ such that } \forall (x, z) \in A, d(y, z) \leq t) \quad \text{and} \quad (\forall t' < t, \forall y \in \mathbb{R}^n, \exists (x, z) \in A \text{ such that } d(y, z) > t').$$

The distance function being subanalytic and subanalytic sets being stable under linear projections, finite union, finite intersection, and complementary, the set of points (x, t) satisfying these two previous conditions are subanalytic.

In fact, F is the intersection of the two sets defined by these two conditions. The quantifiers involved in these conditions may be “eliminated” if one considers the sets as the linear projection or the complementary of the linear projection of some subanalytic set defined in a space of higher dimension. For example, this can be done in the following way for the first of the two sets. Let Π_{xyt} be the canonical projection $(x, z, t, y) \in A \times \mathcal{O} \times \mathbb{R} \rightarrow (x, y, t)$, let Π_{xt} be the canonical projection $(x, y, t) \in A \times \mathbb{R} \rightarrow (x, t)$. The first set is thus defined by the following:

$$\Pi_{xt} \left(\left(\Pi_{xyt} \{ (x, y, z, t) \in A \times \mathcal{O} \times \mathbb{R} : d(z, y) > t \} \right)^c \right).$$

The similar construction, for the second set is left to the reader. So F is a subanalytic set of $\mathbb{R}^n \times [0, +\infty[$. \square

References

- [1] N. Amenta, S. Choi, T. Dey, N. Leekha, A simple algorithm for homeomorphic surface reconstruction, *Int. J. Comput. Geom. Appl.* 12 (1 and 2) (2002) 125–141.
- [2] N. Amenta, S. Choi, R. Kolluri, The power crust, unions of balls and the medial axis transform, *Comput. Geom.: Theory Appl.* 19 (2–3) (2001) 127–153.
- [3] N. Amenta, M. Bern, Surface reconstruction by Voronoi filtering, *Discrete Comput. Geom.* 22 (1999) 481–504.
- [4] D. Attali, J.-D. Boissonnat, H. Edelsbrunner, Stability and computation of the medial axis—a state-of-the-art report, in: T. Möller, B. Hamann, B. Russell (Eds.), *Mathematical Foundations of Scientific Visualization, Computer Graphics, and Massive Data Exploration*, Springer-Verlag, Berlin, 2004.
- [5] M. Berger, *Geometry I*, Universitext Series, Springer-Verlag, Berlin, 1998.
- [6] E. Bierstone, P. Milman, *The local geometry of analytic mappings*, Universita di Pisa, ETS Editrice Pisa, 1988.
- [7] E. Bierstone, P. Milman, Semi-analytic and subanalytic sets, *Publ. Math. I.H.E.S.* 67 (1988) 5–42.
- [8] R. Blanding, C. Brooking, M. Ganter, D. Storti, A skeletal-based solid editor, in: *Proceedings of the Fifth ACM Symposium on Solid Modeling and Applications*, 1999, pp. 141–150.
- [9] F. Cazals, J.D. Boissonnat, Smooth surface reconstruction via natural neighbour interpolation of distance functions, in: *Sixteenth ACM Symposium on Computational Geometry*, 2000, pp. 223–232.
- [10] F. Chazal, R. Soufflet, Stability and finiteness properties of medial axis and skeleton, *J. Control Dyn. Syst.* 10 (2) (2004) 149–170.
- [11] F. Chazal, A. Lieutier, Weak feature size and persistent homology: computing homology of solids in \mathbb{R}^n from noisy data samples, *Rapport de recherche 378*, Institut de Mathématiques de Bourgogne, 2004. Frédéric Chazal Home page <http://math.u-bourgogne.fr/topologie/chazal/publications.htm>.
- [12] F.H. Clarke, *Optimization and NonSmooth Analysis*, Wiley–Interscience, New York, 1983.
- [13] F.H. Clarke, Generalized gradients and applications, *Trans. Am. Math. Soc.* 205 (1975) 247–262.
- [14] T. Culver, J. Keyser, D. Manocha, Accurate computation of the medial axis of a polyhedron, in: *Proceedings of the Fifth ACM Symposium on Solid Modeling and Applications*, 1999, pp. 179–190.
- [15] T.K. Dey, W. Zhao, Approximate medial axis as a Voronoi subcomplex, in: *7th ACM Symposium on Solid Modeling and Applications*, 2002, pp. 356–366.
- [16] T.K. Dey, W. Zhao, Approximating the medial axis from the Voronoi diagram with a convergence guarantee, *Algorithmica* 38 (2004) 179–200.

- [17] T.K. Dey, J. Giesen, M. John, Alpha-shapes and flow shapes are homotopy equivalent, in: Proceedings of the 35rd Annual ACM Symposium on the Theory of Computing (STOC), 2003.
- [18] H. Edelsbrunner, Surface Reconstruction by Wrapping Finite Point Sets in Space, in: B. Aronov, S. Basu, J. Pach, M. Sharir (Eds.), *Discrete and Computational Geometry The Goodman-Pollack Festschrift*, yurinsha 2004, ISBN 3-540-00371-1.
- [19] M. Etzion, A. Rappoport, Computing the Voronoi diagram of a 3-D polyhedron by separate computation of its symbolic and geometric parts, in: Proceedings of the Fifth ACM Symposium on Solid Modeling and Applications, 1999, pp. 167–178.
- [20] M. Etzion, A. Rappoport, Computing Voronoi skeletons of a 3-d polyhedron by space subdivision, *Comput. Geom.: Theory Appl.* 21 (3) (2002) 87–120.
- [21] S. Ferry, When ε -boundaries are manifolds, *Fund. Math.* 90 (1976) 199–210.
- [22] M. Foskey, M.C. Lin, D. Manocha, Efficient computation of a simplified medial axis, in: Proceedings of the Eighth ACM Symposium on Solid Modeling and Applications, 2003, pp. 96–107.
- [23] J.H.G. Fu, Tubular neighborhoods in euclidean spaces, *Duke Math. J.* 52 (4) (1995).
- [24] W. Fulton, *Algebraic Topology, A First Course*. Graduate Texts in Mathematics, Springer-Verlag, Berlin, 1995.
- [25] J. Giesen, M. John, The flow complex: a data structure for geometric modeling, in: Proceedings of the 14th Annual ACM-SIAM Symposium on Discrete Algorithms (SODA), 2003, pp. 285–294.
- [26] K. Grove, Critical point theory for distance functions, *Proc. Symp. Pure Math.* 54 (Part 3) (1993).
- [27] A. Lieutier, Any open bounded subset of R^n has the same homotopy type as its medial axis, *Comput. Aided Design* 36 (2004) 1029–1046.
- [28] S. Lojasiewicz, Sur la Géométrie semi- et sous-analytique, *Ann. Inst. Fourier* 43 (5) (1993).
- [29] W. Massey, *Algebraic Topology: An Introduction*, Harbrace College Mathematics Series, Harcourt, Brace and World, New York, 1967.
- [30] G. Matheron, Examples of topological properties of skeletons (Chapter 11), On the negligibility of the skeleton and the absolute continuity of erosions (Chapter 12), in: Jean Serra (Ed.), *Image Analysis and Math. Morphology*, vol. 2: Theoretical Advances, Academic Press, New York, 1988, pp. 216–256.
- [31] J.R. Munkres, *Elements of Algebraic Topology*, Addison-Wesley, Reading, MA, 1984.
- [32] A. Sheffer, M. Etzion, A. Rappoport, M. Bercovier, Hexahedral Mesh Generation using the Embedded Voronoi Graph, in: 7th International Meshing Roundtable, Sandia National Lab, October, 1998, pp. 347–364.
- [33] K. Suresh, Automating the CAD/CAE dimensional reduction process, in: Proceedings of the Eighth ACM Symposium on Solid Modeling and Applications, 2003, pp. 76–85.